River Flow 2010 - Dittrich, Koll, Aberle & Geisenhainer (eds) - © 2010 Bundesanstalt für Wasserbau ISBN 978-3-939230-00-7

# Two Dimensional Analysis of Flow Patterns and Dispersion in Meandering Channels

I. W. Seo & S. W. Park
*Dept. of Civil and Environmental Engineering, Seoul National University, Seoul, South Korea*

ABSTRACT: In this research, both laboratory and numerical studies were performed to reveal effects of the secondary flow on flow structure and dispersion of pollutant in curved channels. From the analysis of experiments, primary flows and tracer dispersion have been visualized. For the numerical simulation, two-dimensional FEM models, SMS and RAMS, have been applied. Experimental results revealed that, in the S-curved channel with rectangular cross-section, primary flow skews toward the inner bank at the bends whereas, at the crossovers, flow is symmetric. The maximum velocities were occuring along the shortest course of the S-curved channel. The tracer cloud generally follows the path of the maximum velocity. At the first bend, high concentration was detected near the left bank. Passing the crossover, the tracer cloud moves along the centerline of the channel. Then, the tracer cloud moves to the inner bank at the second bend. The numerical simulation showed that simulated velocity vectors are in good agreements with observed data.

*Keywords: Flow structure, Longitudinal and Transverse dispersion, Meandering channel, Secondary flow, 2-D FEM model*

## 1 INTRODUCTION

Rivers and streams have been used for the receiving water of various pollutants from sewage treatment plants and accidental release of toxic materials. Thus, it is necessary to predict accurately the behavior of pollutants which are dispersing and moving with flowing water in the rivers. To simulate complex flow and mass transport in meandering channels, a 3D hydrodynamic model is required. However, for practical engineering problems in shallow and long rivers, a 2D model could be used greatly reducing computational efforts and experimental expenses.

In this research, flow structure and dispersion of pollutant in curved channels were analyzed through laboratory and numerical studies. In the laboratory experiments, flow and tracer dispersion were measured using robust techniques. The numerical simulation was performed using the two-dimensional FEM models.

## 2 RESEARCH BACKGROUND

### 2.1 *Experimental Analysis*

Fischer (1969), for the first time, suggested flow features to the transverse dispersion coefficient considered bend effects. Chang (1971) conducted laboratory experiments with the S-curved channel to obtain the transverse dispersion coefficient considering the secondary flow effects. A theoretical approach which in another methodology for evaluating the transverse dispersion coefficient in cases of having no concentration data was proposed, for the first time, by Fischer (1969) using the transverse velocity equation of Rozovskii (1957). Recently, Boxall and Guymer (2003) suggested new theoretical equation which is derived from the method of Chickendu (1986). Summary of assumptions and results of previous studies which has been involved with this study have been represented in Table 1.

Table 1. Experimental analysis of mixing in channels

| Researcher | Channel | Specific results |
|---|---|---|
| Elder (1959) | Straight | - $e_y / HU_* = 0.23$ |
| Fischer (1969) | Meander | - derived theoretical form |
| Chang (1971) | Meander | - proposed empirical equation |
| Miller & Richardson (1974) | Straight | - $D_L / e_y > 100$ |
| Krisnappan & Lau (1977) | Meander | - $0.222 < D_T / WU_*,\ 0.416 > D_T / WU_*$ |
| Lau & Krisnappan (1977) | Straight | - suggested using $D_T / WU_*$ instead of $D_T / HU_*$ |
| Webel & Schatzmann (1984) | Straight | - criticized results of Lau & Krisnappan (1977) |
| Almquist & Holley (1985) | Meander | - transverse dispersion coefficient increases in natural cross section |
| Nokes & Wood (1988) | Straight | - transverse dispersion coefficient is dependent of a friction factor |
| Boxall & Guymer (2003) | Meander | - conducted with setups natural cross-section |
| Boxall et al. (2003) | Meander | - transverse dispersion coefficient varies in direction of channel curvature |

### 2.2 *Numerical Analysis*

Numerical models have been developed for describing circulation phenomena and the solute transport in the meandering open channel flows. McGuirk and Rodi (1978) developed a depth-averaged model for the near field calculations of the flow and concentration distribution by side discharges of the pollutant into open-channel flow. Duan (2004) derived a dispersion term for the depth-averaged 2D model in Cartesian coordinates and used the Schmidt number as a calibration parameter to simulate mass dispersion in meandering channels. The model by Duan (2004) was applied to the experiments of Chang (1971) to test the capability of the model to simulate mass transport in meandering channels.

## 3 NUMERICAL MODEL

### 3.1 *RAMS*

RAMS (River Analysis and Modeling System) is 2D river flow analysis software package which consists of river flow analysis model (RAM2), pollutant transport model (RAM4), bed elevation change model (RAM6), and graphic user interface (RAMS-GUI). This software can simulate the movements of water, pollutant, and sediment in natural rivers with complex topography by 2D finite element numerical calculations with underlying consistency and generality. This software would provide accurate and stable solutions to open channel flow equation, and mass transport equation for various types of problems. Details about governing equations of RAMS package can be confirmed in website (http://www.rams.or.kr).

Flow model, RAM2, is a finite element model based on Streamline Upwind / Petrov – Galerkin (SU/PG) scheme for analyzing and simulating two-dimensional flow characteristics of irregular natural rivers with complex geometries. The governing equations are

$$\frac{\partial h}{\partial t}+\frac{\partial (uh)}{\partial x}+\frac{\partial (vh)}{\partial y}+i=0 \quad (1)$$

$$\frac{\partial (uh)}{\partial t}+\frac{\partial (u^2 h)}{\partial x}+\frac{\partial (uvh)}{\partial y}+g\frac{\partial (h^2/2a)}{\partial x}=gh(S_{ax}-S_{fx}) \quad (2)$$

$$\frac{\partial (vh)}{\partial t}+\frac{\partial (v^2 h)}{\partial y}+\frac{\partial (uvh)}{\partial x}+g\frac{\partial (h^2/2a)}{\partial y}=gh(S_{ay}-S_{fy}) \quad (3)$$

where $h$ is water depth, $u$ and $v$ are velocities in the $x$, $y$ directions respectively, $i$ is infiltration capacity, $g$ is the gravity acceleration, $S_{ax}$ and $S_{ay}$ are hydraulics .

The type of elements in a mesh can be a triangular, quadrilateral or mixed one. A triangular element could have either 3-nodes or 6-nodes and a quadrilateral element either 4–nodes or 8-nodes. This mesh can be constructed from DEM and TIN format in the tools of GIS.

RAM4 is a FEM model for pollutant transport analysis in two-dimensional flow fields and it is developed based on the depth-averaged mass transport equation. It can calculate the advection and dispersion of injected substances in a two-dimensional flow field. This engine can treat the conservative or non-conservative substances as pollutant tracers.

$$\frac{\partial c}{\partial t}+\nabla\cdot(\mathrm{q}c)-\nabla\cdot(\mathrm{D}\cdot\nabla c)=0 \quad (4)$$

where $c$ is unknown variable which denotes solute concentration in this model, $q$ the fluid velocity vector, and $D$ the diffusion/dispersion tensor.

### 3.2 *RMA-2*

RMA2 and is the 2D depth-averaged finite element hydrodynamic model of commercial soft-

ware SMS (Surface-water modeling system. It computes a finite element solution of the Reynolds form of the Navier-Stokes equations for turbulent flow. Friction is calculated with the Manning's or Chezy equation, and eddy viscosity coefficients are used to define turbulent characteristics. In this model, both steady and unsteady state problems can be simulated. The generalized computer program RMA2 solves the depth-integrated equations of fluid mass and momentum conservation in two horizontal directions. The forms of governing equations are

$$h\frac{\partial u}{\partial t}+hu\frac{\partial u}{\partial x}+hv\frac{\partial u}{\partial y}-\frac{h}{\rho}\left(E_{xx}\frac{\partial^2 u}{\partial x^2}+E_{xy}\frac{\partial^2 u}{\partial y^2}\right)$$
$$+gh\left(\frac{\partial b}{\partial x}+\frac{\partial h}{\partial x}\right)+\frac{gun^2}{h^{1/3}}U-\zeta V_a^2\cos\psi-2h\omega v\sin\varphi_l \quad (5)$$
$$=0$$

$$h\frac{\partial v}{\partial t}+hu\frac{\partial v}{\partial x}+hv\frac{\partial v}{\partial y}-\frac{h}{\rho}\left(E_{yx}\frac{\partial^2 v}{\partial x^2}+E_{yy}\frac{\partial^2 v}{\partial y^2}\right)$$
$$+gh\left(\frac{\partial b}{\partial y}+\frac{\partial h}{\partial y}\right)+\frac{gvn^2}{h^{1/3}}U-\zeta V_a^2\sin\psi+2h\omega v\sin\varphi_l \quad (6)$$
$$=0$$

$$\frac{\partial h}{\partial t}+h\left(\frac{\partial u}{\partial x}+\frac{\partial v}{\partial y}\right)+u\frac{\partial h}{\partial x}+v\frac{\partial h}{\partial y}=0 \quad (7)$$

where $\rho$ is density of fluid, $E_{xx}$ is eddy viscosity coefficient for normal direction on $x$ axis surface, $E_{yy}$ is for normal direction on $y$ axis surface, $E_{xy}$ and $E_{yx}$ is for shear direction on each surface, $g$ is acceleration due to gravity, $b$ is elevation of bottom, $n$ is roughness coefficient in Manning's formula, $\zeta$ is empirical wind shear coefficient, $V_a$ is wind speed, $\omega$ is rate of earth's angular rotation, and $\phi_l$ is local latitude.

## 4 EXPERIMENTS

### 4.1 *Laboratory Setup*

In this study, flow and tracer experiments were conducted in the S-curved meandering laboratory channel with a rectangular cross-section which is 16.5 m long, 1 m wide, and 0.6 m high. It consists of two circular bends connected by straight sections as shown in Figure 1. The radius of curvature of the bend region is 2.0 m, the wavelength is 7.5 m, and the arc angle is 150°. Meander properties of the laboratory channel were selected considering previous studies which are listed in Table 2. Velocity and solute concentration were measured by micro-ADV (Acoustic Doppler Velocimetry) and the electrode conductivity meter respectively. As the tracer, salt solution was used. The density of the salt solution was adjusted to that of the flume water by adding methanol. The tracer solution can be instantaneously injected into water flow as a full-depth vertical line source by using the instantaneous injecting cylinder. The initial concentration of the tracer was 100,000 mg/ℓ. The interval of concentration measuring points at each section was about 7 cm in the transverse direction. Vertically, concentration was measured at a point located 60 % of the depth above the bottom for shallow water conditions ($H$ = 15, 20 cm). For deep water conditions ($H$ = 30, 40 cm), concentration was measured at two points, 20 % and 80% of the depth above the bottom. Total of 12 cases of tracer tests were performed as listed in Table 3.

Table 2. Properties of meander pattern of previous and this research

| Researcher | $R_C$/W | $\theta$(°) | $\lambda/W$ | $\lambda/R_C$ | *Sin.* |
|---|---|---|---|---|---|
| Leopold & Wolman (1960) | 2.3 | - | 10.9 | 4.7 | - |
| Chang (1971) | 3.6 | 90 | - | - | *1.11* |
| Krishnappan & Lau (1977) | 0.6 ~ 2.2 | - | 6.3 | 3 ~ 10.8 | - |
| Almquist & Holley (1985) | 3 | 125 | 12 | 4 | *1.30* |
| Guymer (1998) | 3.5 | 120 | 13.7 | 3.9 | *1.21* |
| Seo et al. (2004) | 2.4 | 120 | 9.7 | 4 | *1.32* |
| *This study* | *2.0* | *150* | *7.5* | *3.8* | *1.52* |

Table 3. Hydraulic conditions

| Case | $h$ (cm) | $\bar{u}$ (cm/s) | $Q$ (ℓ/s) | *Fr* |
|---|---|---|---|---|
| B151 | 15 | 10 | 15 | 0.08 |
| B152 | 15 | 20 | 30 | 0.16 |
| B153 | 15 | 40 | 60 | 0.33 |
| B201 | 20 | 7.5 | 15 | 0.05 |
| B202 | 20 | 15 | 30 | 0.11 |
| B203 | 20 | 30 | 60 | 0.21 |
| B301 | 30 | 5 | 15 | 0.03 |
| B302 | 30 | 10 | 30 | 0.06 |
| B303 | 30 | 20 | 60 | 0.12 |
| B401 | 40 | 3.75 | 15 | 0.02 |
| B402 | 40 | 7.5 | 30 | 0.04 |
| B403 | 40 | 15 | 60 | 0.08 |

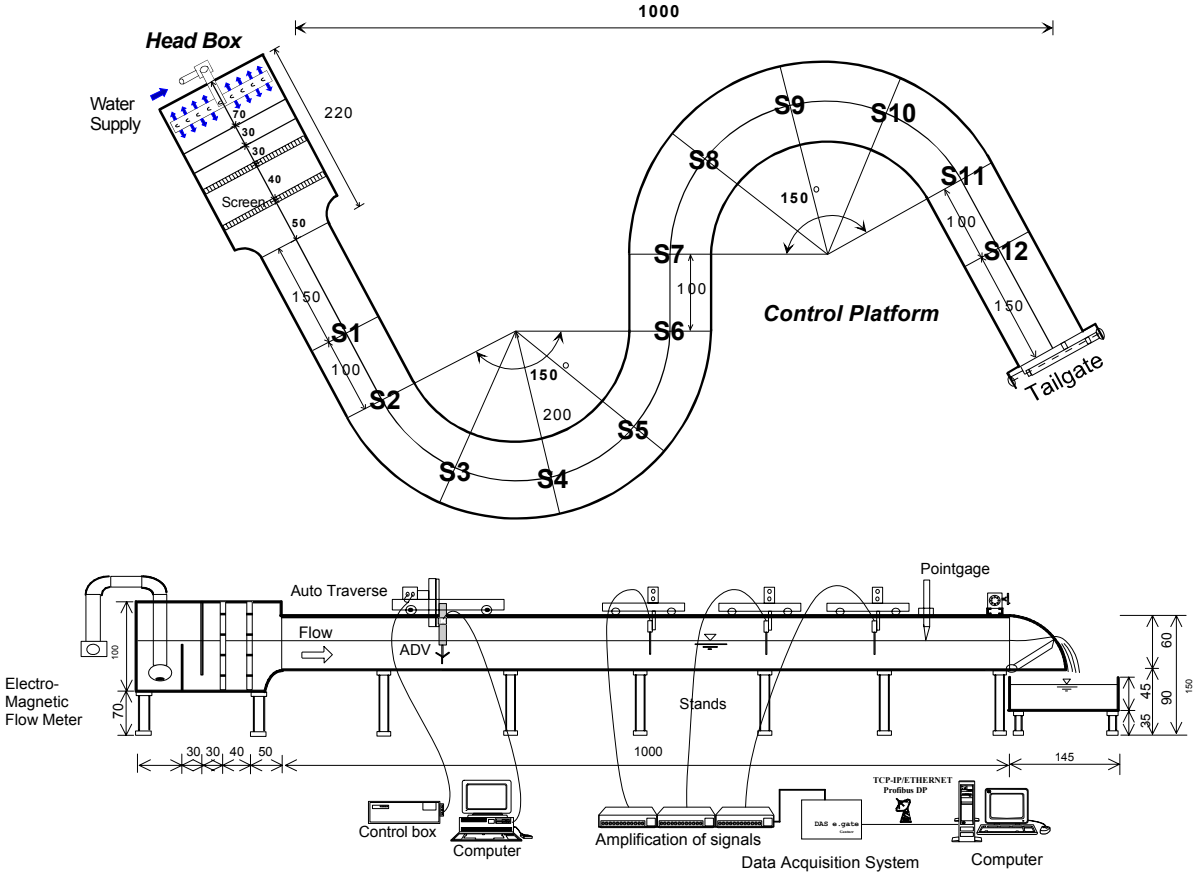


Figure 1. Sketches of S-curved laboratory channel (upper: plan view, lower: side view; unit: cm)

## 4.2 *Experimental Results*

In Figure 2, velocity data detected in the S-curved channel were expressed by two dimension-al vector profiles at the test sections (S1~S12). In this figure, it is noteworthy that transverse distribution of the primary velocity skews toward the inner bank at the bends and at the crossovers, al-most symmetric. The maximum velocities in each transverse section were detected along the shortest course of the channel. This flow pattern is opposite to the flow characteristics found in the natural meandering channels. The reason of this discrepancy in the flow pattern is that experiments were conducted on the rectangular cross-section channel, whereas the cross-sectional shape of the natural stream is usually triangular, and skewed to the outer bank.

In Figure 3, contours of the concentration tracer cloud for Case B202 (H = 20 cm, Q = 30 ℓ/sec) were plotted. In the tracer tests, concentration data were collected at the sampling points as a function of time. All concentration data were filtered by the moving average to reduce the mechanical noise. In order to visualize the behavior of the tracer clouds, the spatial contours which were made by the interpolation technique through the concentration-time data were generated.

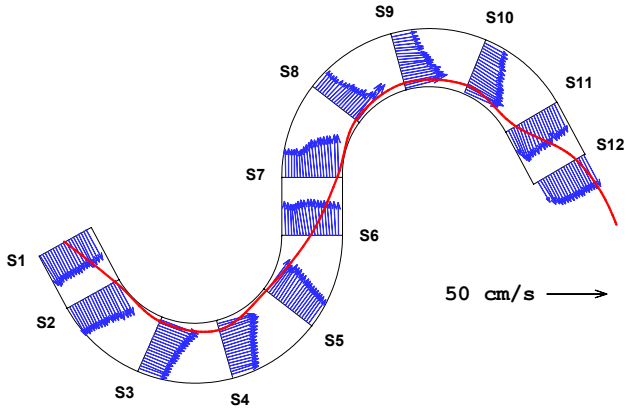


a) Case B202

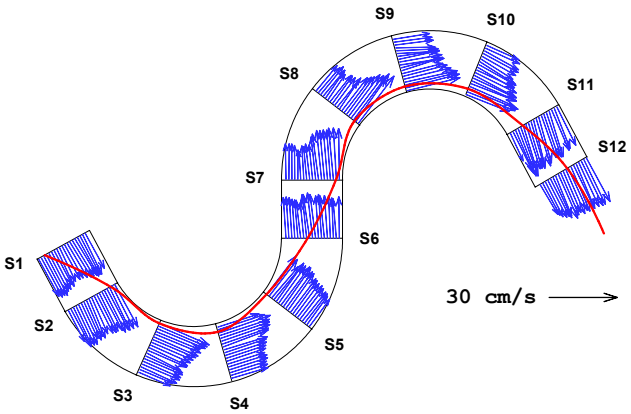


b) Case B302

Figure 2. Vector maps of primary velocity profiles

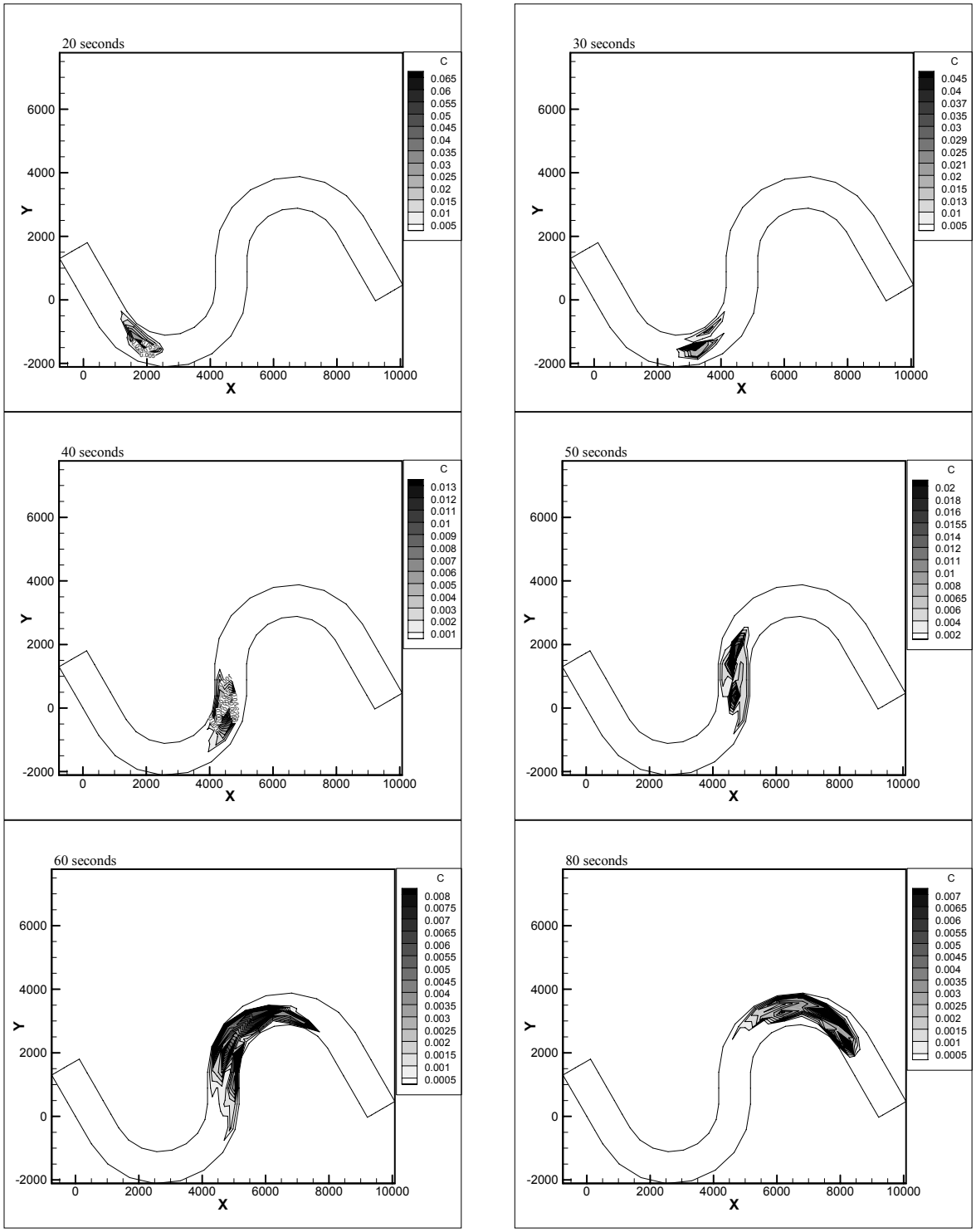


Figure 3. Concentration contours of tracer cloud in case B202 ($H$= 20 cm)

Figure 3 illustrated that entering the first bend, high concentration was detected near the left (inner) bank. At the first apex, the tracer cloud separates into two parts and the main part skews toward the left bank which is the inner bank in the first bend. The residual part remains the outer bank. Passing the crossover between the first bend and second bend, the tracer cloud moves along the centerline of the channel. Then, entering the second bend, again, high concentration was observed near the inner bank. Based on this finding, it could be maintained that even through tracer cloud travels following the maximum primary flow, it separates both in longitudinal and transverse directions due to alternating secondary currents. Thus, secondary flow effects should be incorporated in the estimation of longitudinal and transverse dispersion coefficients.

## 5 NUMERICAL SIMULATIONS

In this study, flow characteristics of the S-curved channel were analyzed using numerical models, RAM2 and RMA-2. Meshes for numerical simula-

tion were given in Figure 4, and propertied of the meshes were listed in Table 4.

In Figure 5, vector maps along with contours of two dimensional primary velocities were plotted. This figure showed that simulated results are in good agreements with observed velocity data given in Figure 2. In this figure, one can find that the primary flow skews toward the inner bank at the bends. At the crossovers, flow is almost symmetric. Thus, in this figure, the maximum velocities were found along the shortest course of the channel.

Magnitudes of primary flow of the simulated and observed results at the first bend (S4) and second bend (S9) were compared in Figure 6. In this figure, predicted values by both models are in good agreements with the experimental data in the apex of the bends even though RMA-2 model overestimates the experimental result while RAM2 model underestimates it.

Table 4. Properties of geometries (RAM2, RMA-2)

| | RAM2 | RMA-2 |
|---|---|---|
| Nodes | 2625 | 7729 |
| Element | 2480 | 2480 |
| Element type | Rectangular (linear basis element) | Rectangular (quadratic basis element) |

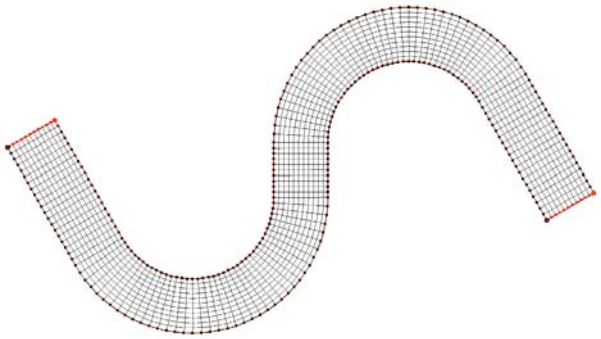

a) RAMS

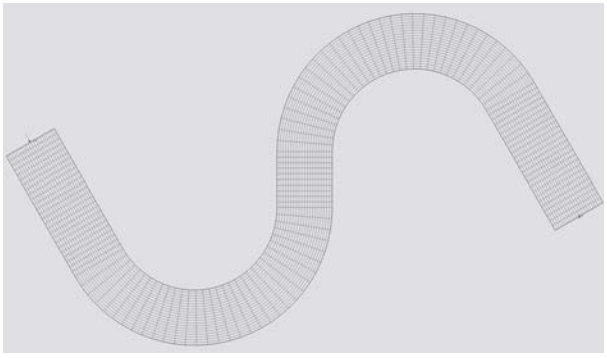

b) SMS

Figure 4. Meshes for simulation with FEM

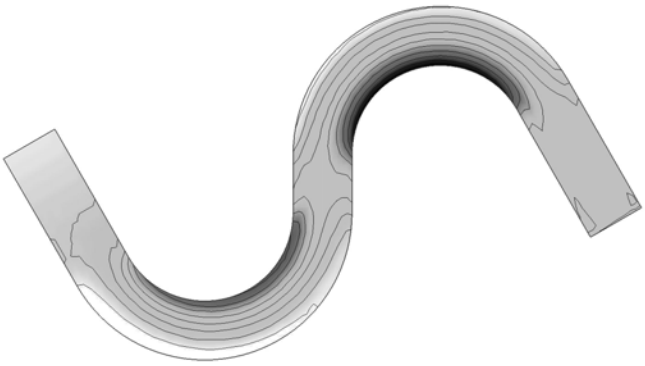

a) Velocity profile using RAM2

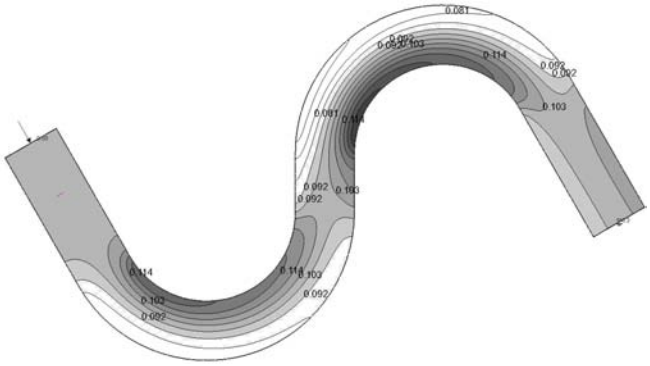

b) Velocity profile using RMA-2

Figure 5. Vector maps of velocity profiles

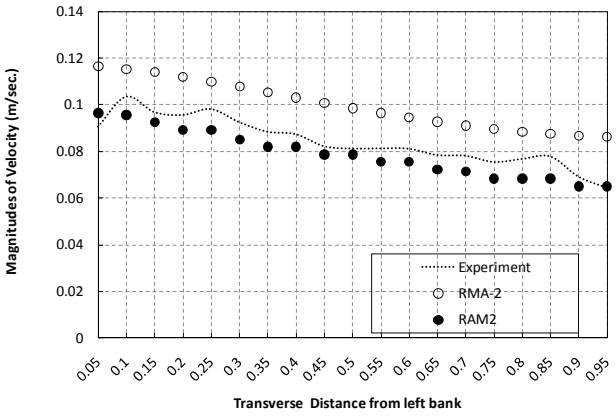


a) Comparison of primary flow at the first bend (S4)

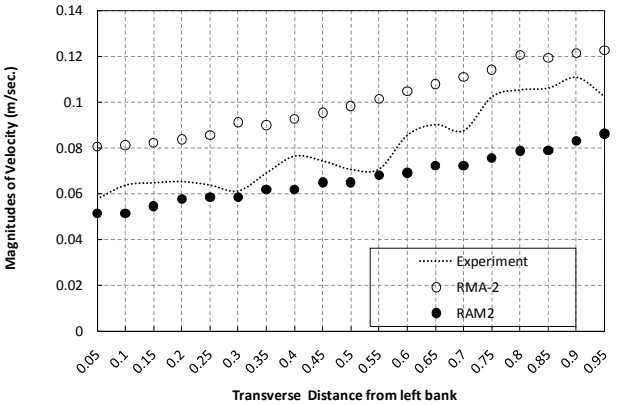


b) Comparison of primary flow at the second bend (S9)

Figure 6. Analysis of velocity data

## 6 CONCLUSIONS AND FUTURE WORKS

In this research, flow and dispersion characteristics in the curved channel were investigated by experiments and numerical models. Flow experiments revealed that, in the S-curved channel with rectangular cross-section, primary flow skews toward the inner bank at the bends whereas, at the crossovers, flow is symmetric. Further, the maximum velocities were found along the shortest course of the S-curved channel. The dispersion experiments illustrated that the tracer cloud generally followed the path of the maximum velocity. At the first bend, high concentration was detected near the left bank. Passing the crossover, the tracer cloud moves along the centerline of the channel. Then, entering the second bend, again, high concentration was observed near the inner bank.

The numerical simulation showed that simulated results are in good agreements with observed velocity data. The predicted values by both models are in good agreements with the experimental data in the apex of the bends even though RMA-2 model overestimates the experimental result while RAM2 model underestimates it.

## ACKNOWLEDGEMENTS

This research was supported by SNU SIR Group of the BK21 research Program funded by Ministry of Education & Human Resources Development and 21C Frontier project "Application of RAMS" of the Ministry of the Science and Technology.

## REFERENCES

Almquist, C. W., and Holley, E. R. 1985. "Transverse mixing in meandering laboratory channels with rectangular and naturally varying cross sections," Technical Report CRWR-205, Univ. of Texas, Austin, Texas.

Boxall, J. B., Guymer, I. 2003. "Analysis and prediction of transverse mixing coefficients in natural channels." Journal of Hydraulic Engineering, ASCE, 129(2), 129-139.

Chang, Y. 1971. Lateral mixing in Meandering Channels. Ph.D. Thesis, University of Iowa.

Duan, G. 2004. "Simulation of flow and mass dispersion in meandering channels." Journal of Hydraulic Engineering, ASCE, 130(10), 964-976.

Elder, J. W. 1959. "The dispersion of marked fluid in turbulent shear flow." J. of Fluid Mech., 5: 544-560.

Fischer, H. B. 1966. "Longitudinal dispersion in laboratory and natural streams." Technical Report KH-R-12, Caltech, Pasadena, California.

Fischer, H. B. 1969. "The effect of bends on dispersion in streams." Water Resour. Res., 5(2), 496-506.

Fischer, H. B., List, E. J., Koh, R. C. Y., Imberger, J., and Brooks, N. H. 1979. Mixing in Inland and Coastal Waters.

Guymer, I. 1998. "Longitudinal dispersion in sinuous channel with changes in shapes." Journal of Hydraulic Engineering, ASCE, 124(1), 33-40.

Krishnappan, B. G., and Lau, Y. L. 1977. "Transverse mixing in meandering channels with varying bottom topography." J. Hydr. Res., IAHR, 15(4): 351-371.

Lau, Y. L., and Krishnappan, B. G. 1977. "Transverse dispersion in rectangular channel." J. Hydr. Div., ASCE, 103(HY10): 1173-1189.

Leopold, L. B., and Wolman, M. G. 1960. "River meanders." Bulletin of the Geological Society of America, 71: 769-794.

McGuirk, J. J., and Rodi, W. 1978. "A depth-averaged mathematical model for the near field of side discharges into open channel flow." Journal of Fluid Mechanics, 86(4), 761-781.

Miller, A. C., and Richardson, E. V. 1974. "Diffusion and dispersion in open channel flow." J. Hydr. Div., ASCE, 100(HY1): 835-847.

Nokes, R. I., and Wood, I. R. 1988. "Vertical and lateral turbulent dispersion: Some experimental results." J. Fluid Mech., 187: 373-394.

Seo, I. W., Baek, K. O., and Jeong, S. J. 2004. "Evaluation of Transverse Dispersion Coefficients in Meandering Channel Under Unsteady Concentration Conditions," Advances in Hydro-Science and -Engineering, Proceedings of 6th International Conference on Hydro-Science and -Engineering, Brisbane, Australia, May 31-June 3.

Webel, G., and Schatzmann, M. 1984. "Transverse mixing in open channel flow." J. Hydr. Engrg., ASCE, 110(4): 423-435.